

**Figure S1**

**Figure S1. HA Tag Sequence Insertion by HDR-Mediated Genome Editing, Related to Figure 1**

(A–J) Confocal microscopic images of brain sections of Cas9 mice showing DAPI signal (blue), EGFP fluorescence (magenta), or immunoreactivities for TH, NeuN or calbindin (magenta) and the HA tag (green) fused to the N-terminus of endogenous CaMKII $\alpha$  (A, B; right, C, D, E; middle and right, and G) or  $\beta$ -Actin (B; left, E; left, F, and H–J). Representative images of brain sections of hippocampus (H), cerebellum (I), and retina (J) transduced with AAV-HDR at E10 (left), E12 or E14 (middle), and E16 (right) are shown.

Scale bars, 50  $\mu$ m.

See also Table S1.

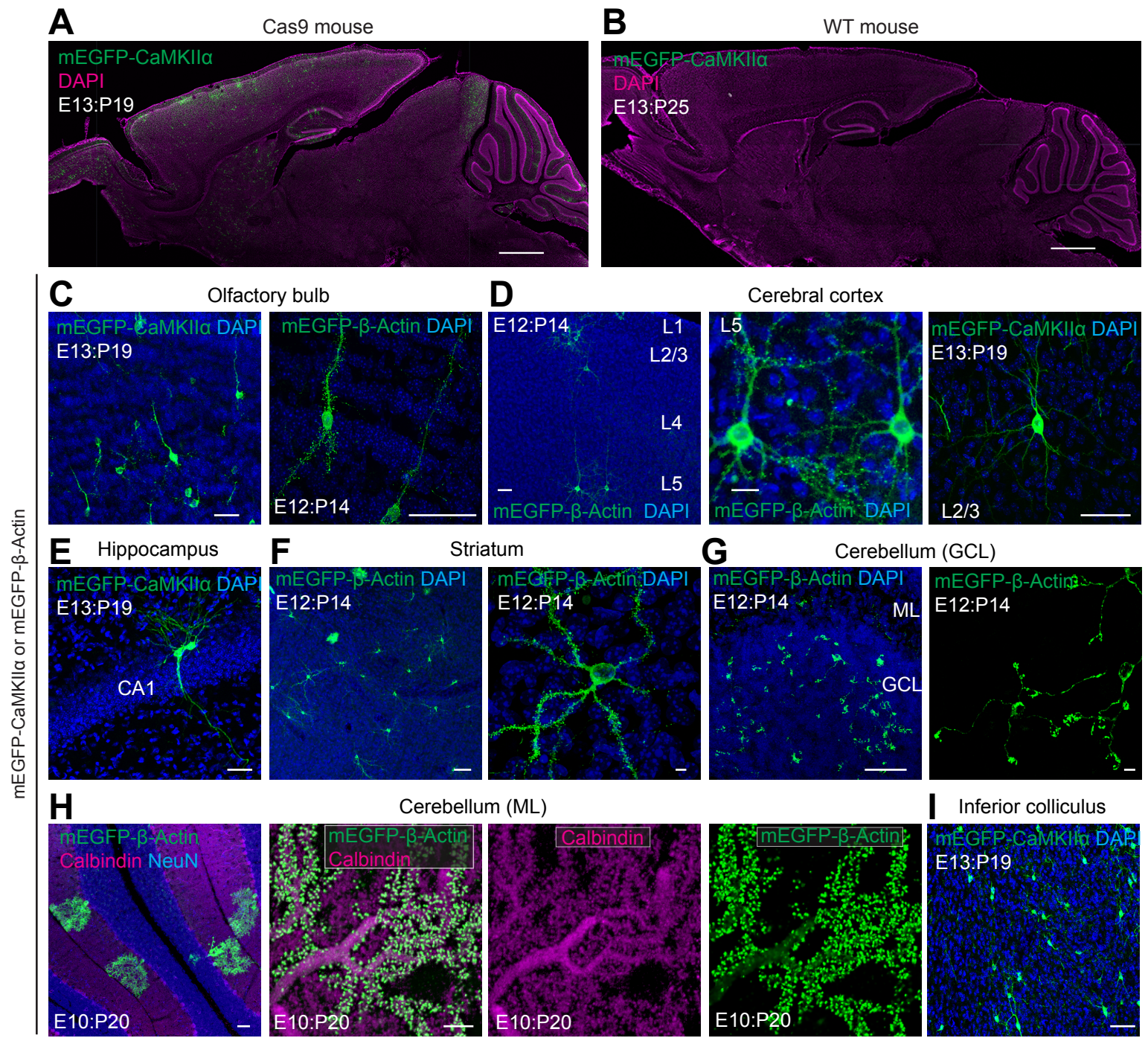


Figure S2

**Figure S2. mEGFP Sequence Insertion by HDR-Mediated Genome Editing, Related to Figure 1**

(A) Confocal microscopic images of whole sagittal brain sections of Cas9 (A) and wild type (B) mice showing mEGFP fluorescence (green) fused to the N-terminus of endogenous CaMKII $\alpha$  and immunoreactivity for NeuN (magenta).

(C–I) Confocal microscopic images of brain sections of Cas9 mice showing DAPI signal (blue), mEGFP fluorescence (green) fused to the N-terminus of endogenous CaMKII $\alpha$  (C; left, D; right, E, and I) or  $\beta$ -Actin (C; right, D; left and middle, F, G, and H), and immunoreactivities for NeuN and calbindin (magenta). L, cortical layer (D); ML, molecular layer; GCL, granule cell layer (G and H).

Scale bars, 1 mm (A); 50  $\mu$ m (C, D; left and right, E, F; left, G; left, H; left, and I); 5  $\mu$ m (D; middle, F; right, G; right, and H; middle and right).

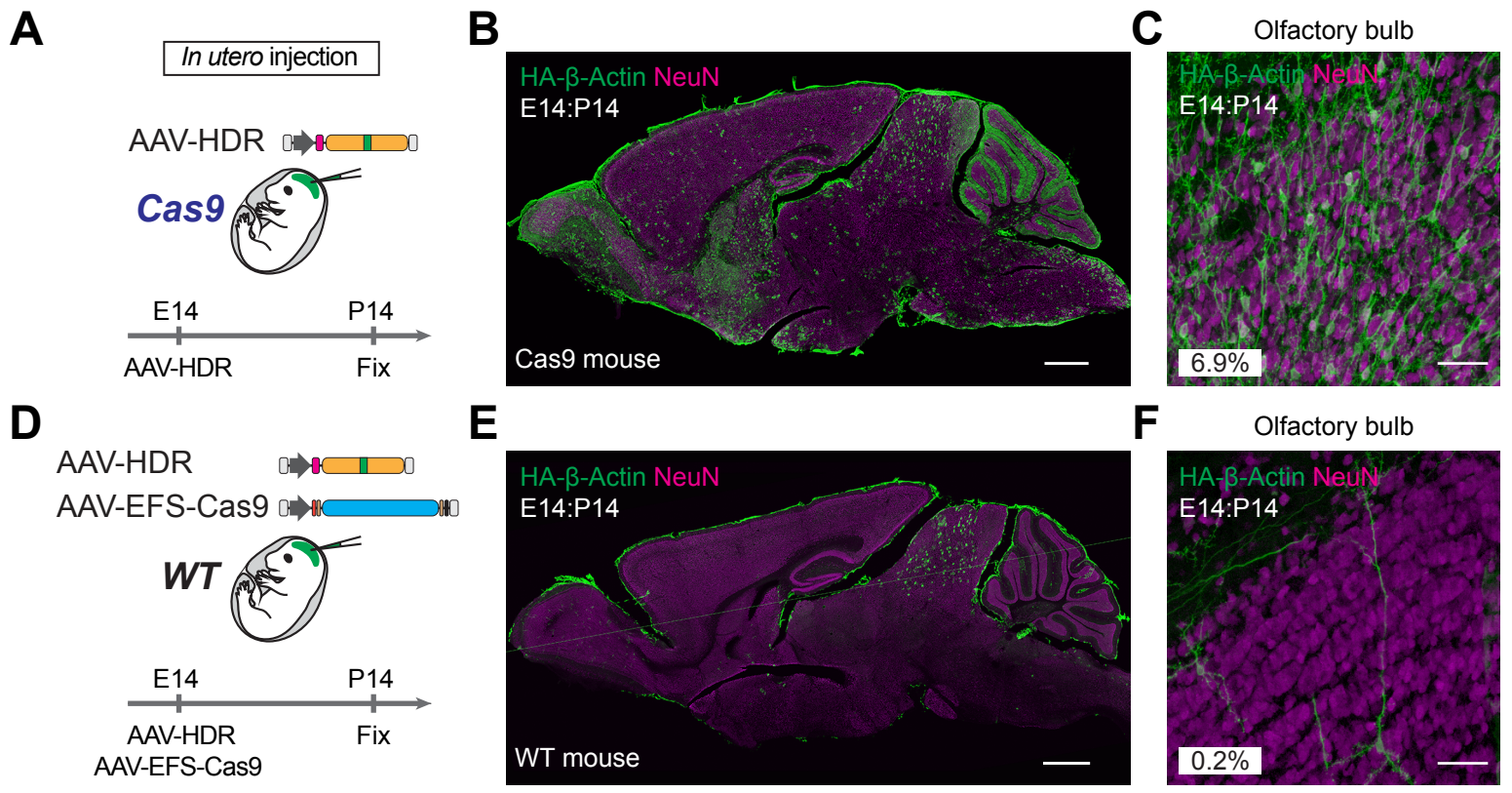


Figure S3

**Figure S3. Comparison of HDR Efficiency between Single and Dual AAV System in the Embryonic Mice Brain, Related to Figure 1 and 4**

(A and D) Schematic illustrations of experiments.

(B, C, E, and F) Confocal microscopic images of brain sections of Cas9 mice injected with AAV-HDR (B and C) and wild type mice injected with AAV-HDR and AAV-EFS-Cas9 (E and F) showing immunoreactivities for NeuN (magenta) and HA tag (green) fused to the N-terminus of endogenous  $\beta$ -Actin. Representative images and knockin efficiency in the granule cell layer of the olfactory bulb are shown (C and F) ([olfactory bulb] single AAV system, HA/NeuN:  $6.9 \pm 1.7\%$ ,  $n = 1910$  cells / 3 slices; dual AAV system, HA/NeuN:  $0.2 \pm 0.1\%$ ,  $n = 2861$  cells / 3 slices).

Scale bars, 1 mm (B and E); 50  $\mu\text{m}$  (C and F).

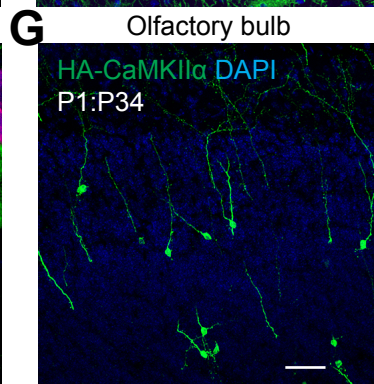
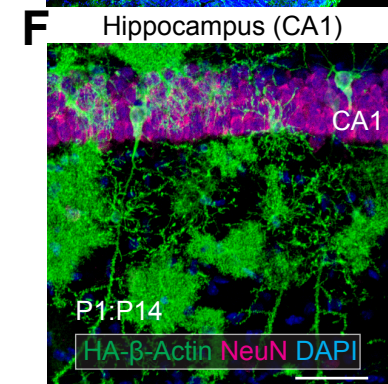
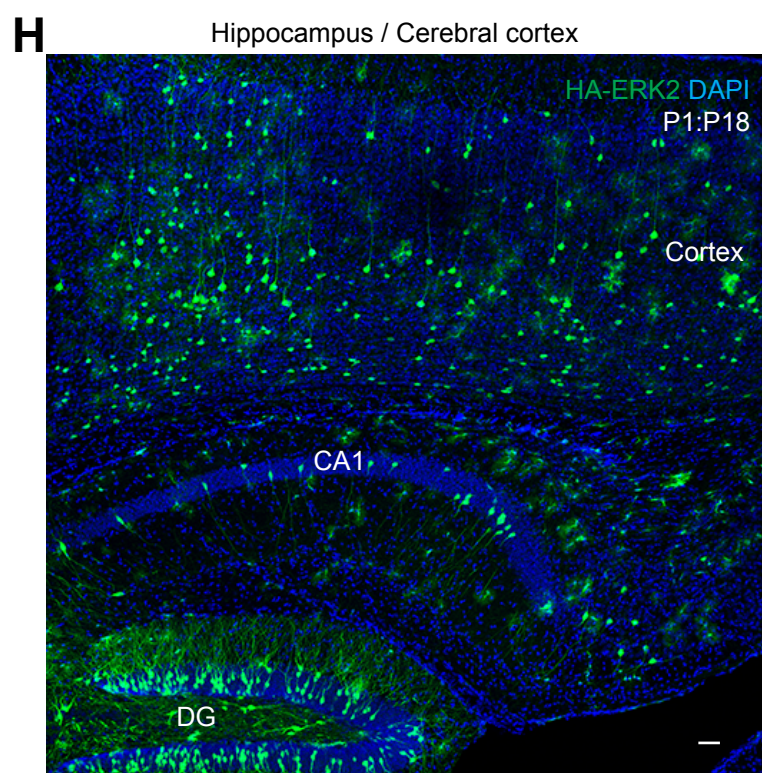
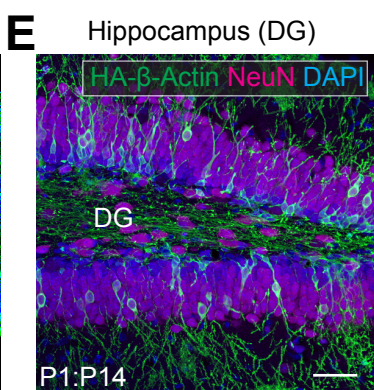
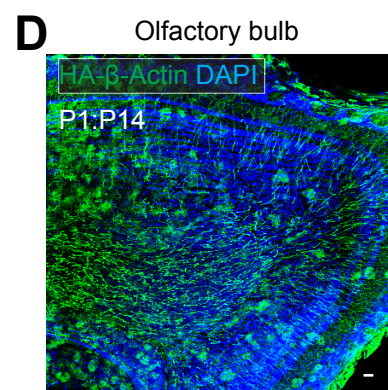
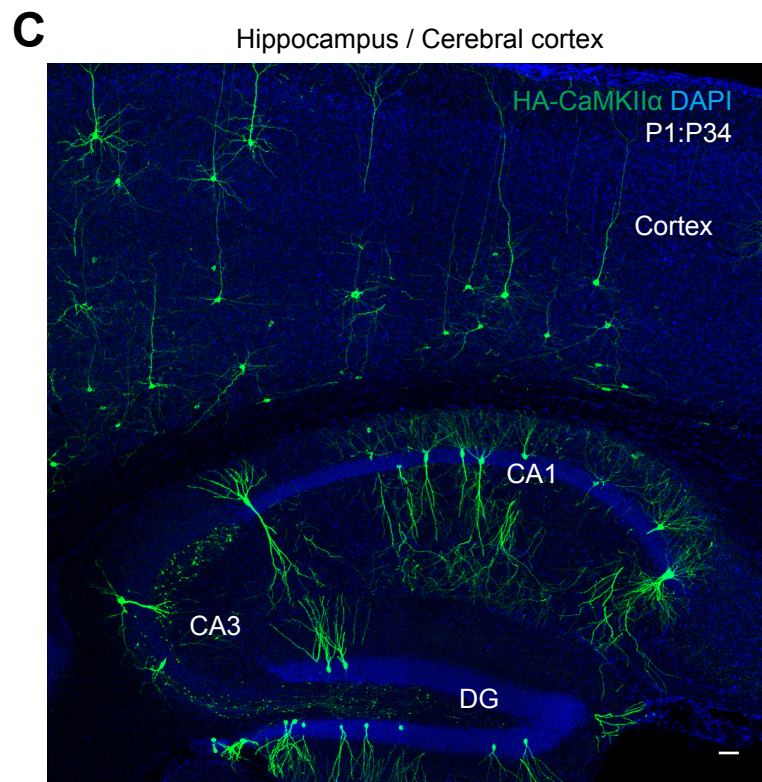
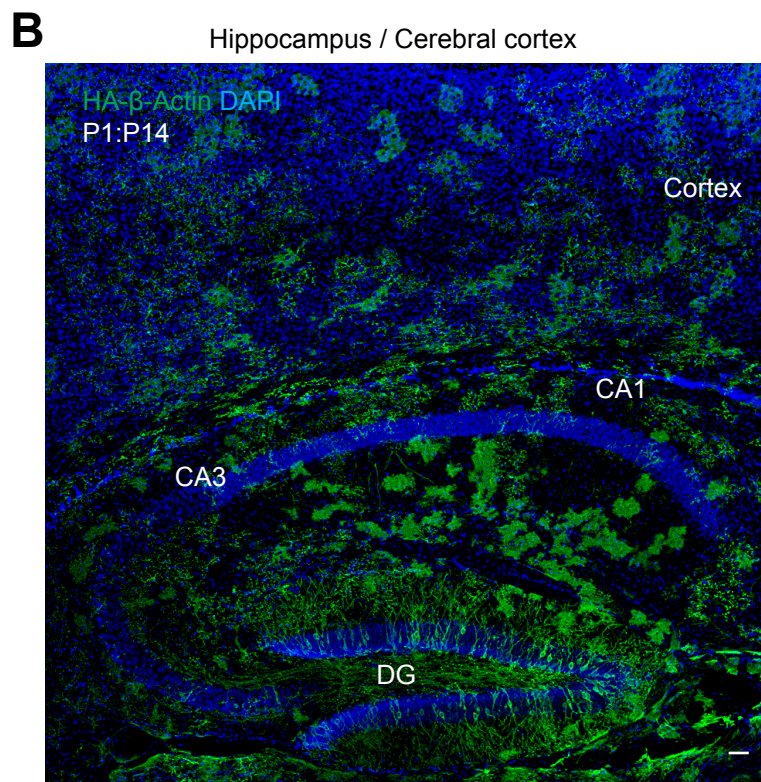
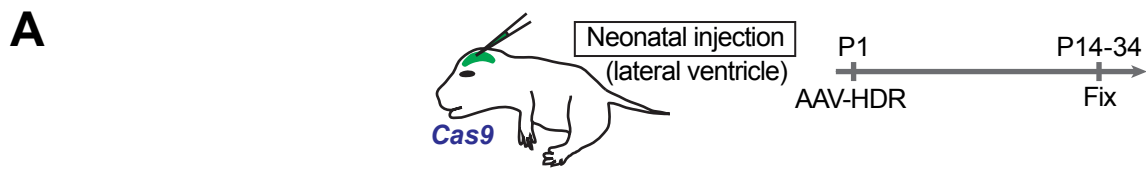


Figure S4

**Figure S4. HDR-Mediated Genome Editing in Mitotic and Postmitotic Cells by Neonatal Intraventricular Injection, Related to Figures 1 and 2**

(A) Schematic illustration of experiments.

(B–H) Confocal microscopic images of brain sections of the cortico-hippocampal regions (B, C, and H), olfactory bulb (D and G), and dentate gyrus (E) and CA1 (F) in the hippocampus showing DAPI signal (blue) and immunoreactivities for NeuN (magenta) and the HA tag (green) fused to the N-terminus of endogenous  $\beta$ -Actin (B, D, E, and F), CaMKII $\alpha$  (C and G), and ERK2 (H).

Scale bars, 50  $\mu$ m.



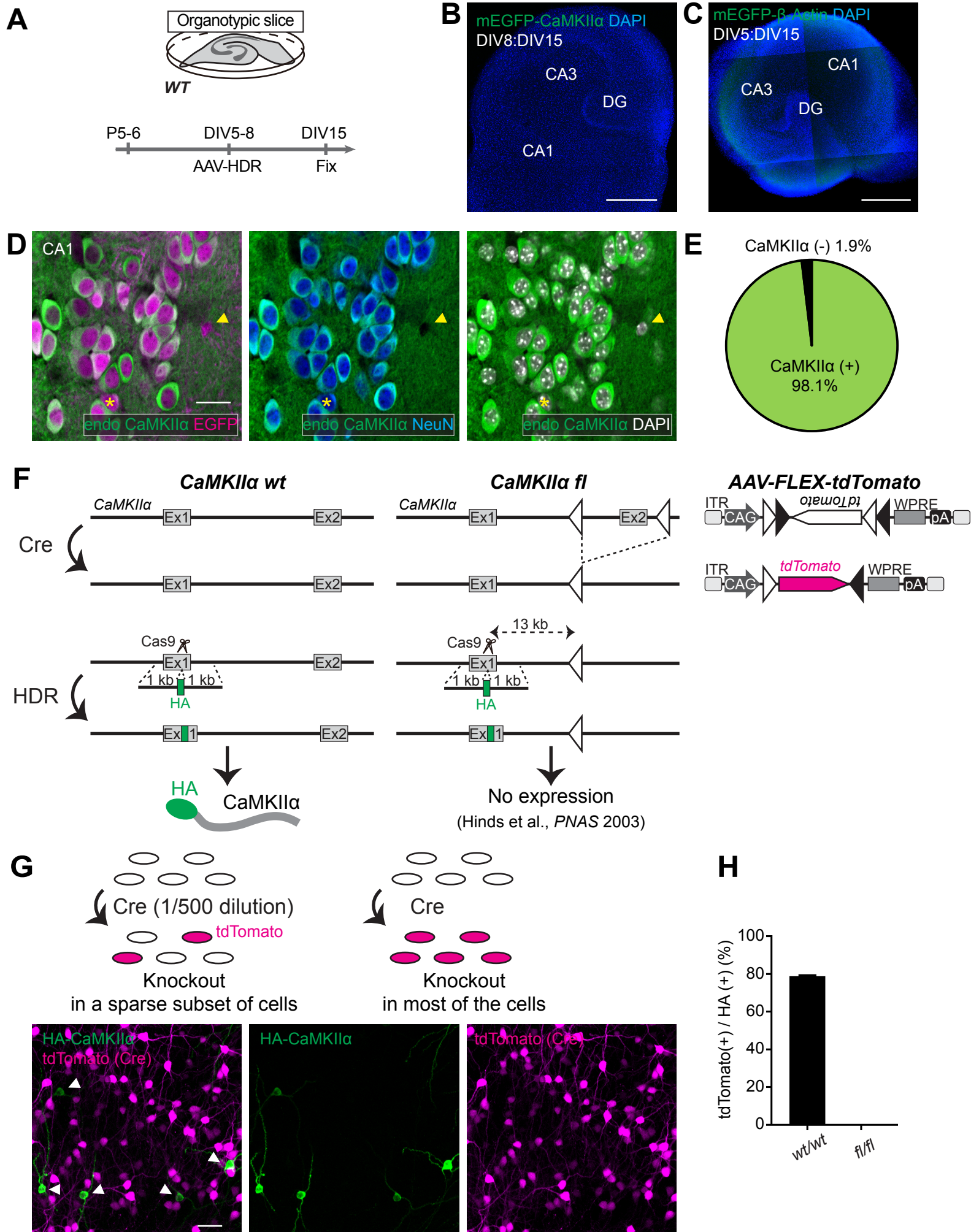


Figure S5

**Figure S5. Verification of Specificity of AAV-Mediated Genome Editing, Related to Figures 2 and 4**

(A) Schematic illustration of experiments.

(B and C) Confocal microscopic images of organotypic hippocampal slice cultures of wild type mice transduced with AAV-HDR for mEGFP-CaMKII $\alpha$  (B) and mEGFP- $\beta$ -Actin (C), showing the DAPI signal (blue) and mEGFP fluorescence (green) fused to the N-terminus of endogenous CaMKII $\alpha$  and  $\beta$ -Actin.

(D) Confocal microscopic images of organotypic hippocampal slice cultures of Cas9 mice transduced with AAV-HDR for HA-CaMKII $\alpha$ , showing the EGFP fluorescence (magenta), DAPI signal (white), and immunoreactivities for the endogenous CaMKII $\alpha$  (green) and NeuN (blue). Yellow asterisk, CaMKII $\alpha$  deleted cell (EGFP-positive, CaMKII $\alpha$ -negative, NeuN-positive cell); yellow arrowhead, non-neuronal cell (EGFP-positive, CaMKII $\alpha$ -negative, NeuN-negative cells).

(E) The ratio of CaMKII $\alpha$  positive and negative cells in all infected neurons is shown (n = 53 cells).

(F) Graphical representation of the mouse genomic loci of *CaMKII $\alpha$*  in wild type (left) and floxed (middle) mice. A sequence of 4 kb containing exon 2 is excised out by Cre recombinase only in floxed mice (upper). Thus, although the HA sequence is inserted by HDR in both genotypes (lower), CaMKII $\alpha$  protein is expressed only in wild type mice. Schematic of AAV-FLEX-tdTomato (right). The inverted tdTomato sequence is re-inverted by Cre recombinase so that tdTomato can serve as a Cre reporter. Open triangle, loxP; filled triangle, lox2272.

(G) AAV-Cre is diluted to 1/500 so that CaMKII $\alpha$  is knocked out in a sparse subset of cells, while CaMKII $\alpha$  is deleted in most of the cells with the original concentration of AAV-Cre.

Confocal microscopic images of organotypic hippocampal slice cultures prepared from CaMKII $\alpha$  conditional knockout mice showing the tdTomato fluorescence (magenta) and immunoreactivity for the HA tag (green) fused to the N-terminus of endogenous CaMKII $\alpha$ . Because CaMKII $\alpha$  is deleted in a sparse subset of cells (tdTomato-positive), HA-positive neurons can be found (white arrowheads), although the HA-positive neurons are all tdTomato-negative.

(H) Summary data on the ratio of the number of tdTomato and HA double-positive cells to HA-positive cells in wild-type (n = 95 cells, 3 slices) and floxed (n = 16 cells, 3 slices) mice.

Scale bar, 50  $\mu$ m (B–D and G).

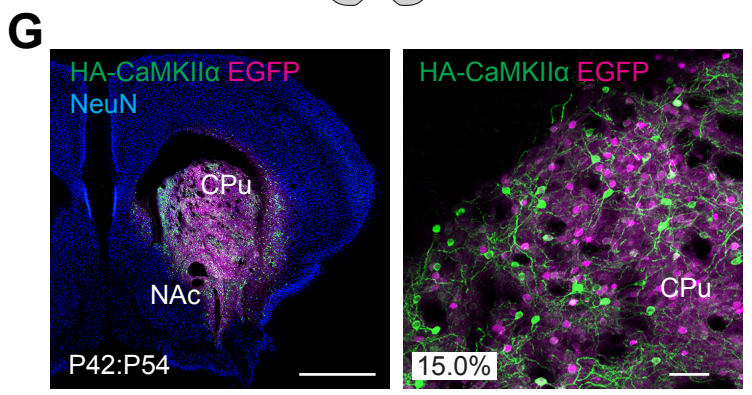
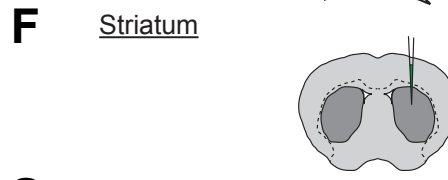
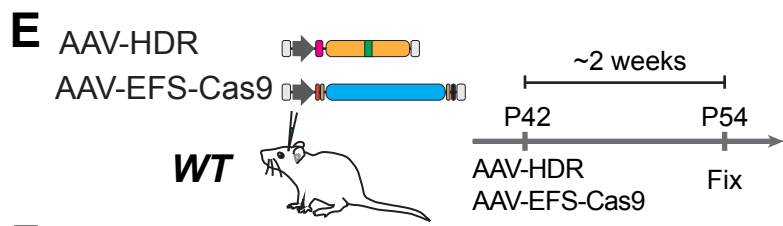
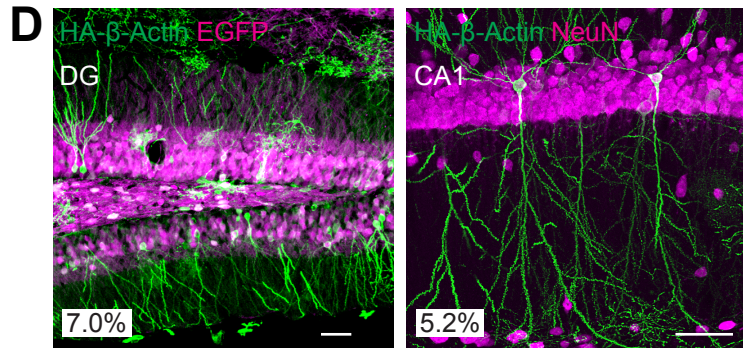
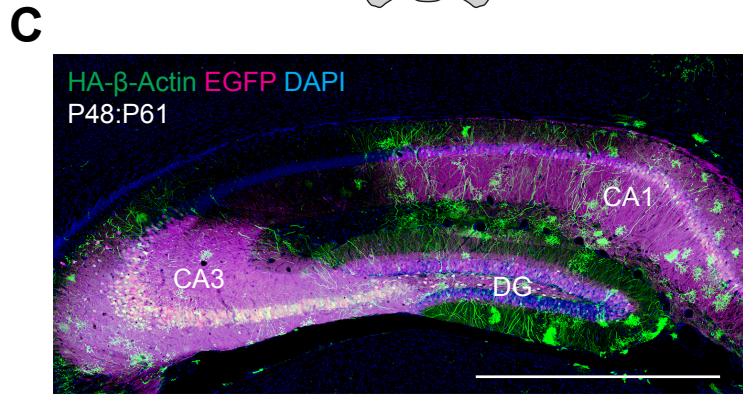
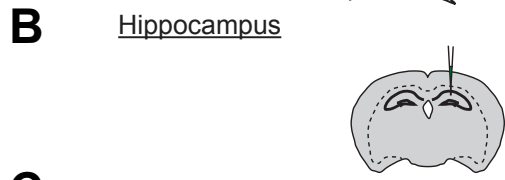
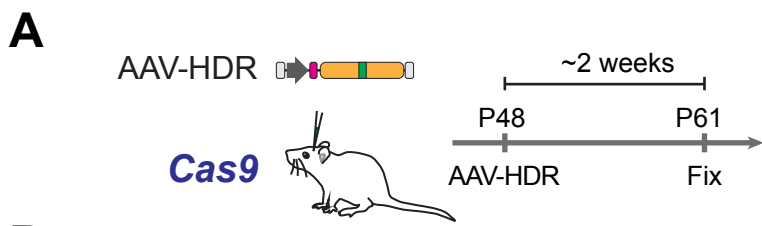


Figure S6

**Figure S6. HDR-Mediated Genome Editing *In Vivo*, Related to Figure 5**

(A and E) Schematic illustrations of experiments.

(B and F) Schematic illustrations of AAV injection sites.

(C, D, and G) Confocal microscopic images of coronal brain sections of the hippocampus of

Cas9 mice injected with AAV-HDR (C and D) and striatum of wild type mice injected with

AAV-HDR and AAV-EFS-Cas9 (G) showing the EGFP fluorescence (magenta) and

immunoreactivities for the HA tag (green) fused to the N-terminus of endogenous  $\beta$ -Actin (C and

D) and CaMKII $\alpha$  (G).

Scale bars, 50  $\mu$ m (D and G; right); 1 mm (C and G).

	E10	E12 or E14	E16
<b>Hippocampus : HA/NeuN (%)</b>			
CA1 pyramidal neurons	10.4 ± 1.6 (496)	1.4 ± 0.1 (657)	0.2 ± 0.2 (647)
DG granule cells	8.5 ± 0.4 (1828)	5.1 ± 0.7 (1685)	12.1 ± 1.8 (1788)
<b>Cerebellum: HA/Calbindin (%)</b>			
Purkinje cells	17.5 ± 1.8 (238)	0.0 ± 0.0 (243)	0.0 ± 0.0 (238)
<b>Retina : HA/NeuN (%)</b>			
Ganglion cells	18.6 ± 2.6 (149)	0.0 ± 0.0 (257)	0.0 ± 0.0 (182)

**Table S1. Spatiotemporal Regulation of Genome Editing Efficiency in Distinct Cell-types Regulated by the Timing of AAV-HDR Administration, Related to Figures S1.**

The numbers of cells analyzed are indicated in parentheses.





	Name	Sequence (5'>3')	Source
<b>sgRNA target sequence</b>	$\beta$ -Actin	tgtgtcttgatagttcgcca	Mikuni et al., 2016
	CaMKII $\alpha$	ctgcctgcccagtgccagga	Mikuni et al., 2016
	ERK2	cggcggctgtgcagccaaca	This study
<b>Genomic PCR primer</b>	HA-F	cccatacgatgttccagatt	Mikuni et al., 2016
	HA-R	gcgtaatctggaacatcgtatg	Mikuni et al., 2016
	GFP-F	catggtcctgctggagttcgtg	This study
	GFP-R	gctgaacttgaggccgtttac	This study
	$\beta$ -Actin-F	ttcacctgccctgagtgttc	This study
	$\beta$ -Actin-R	gggagagcatagccctcgta	This study
	CaMKII $\alpha$ -F	agcacaagcagaaactggga	This study
	CaMKII $\alpha$ -R	tgaatcgggtgcaggtgatg	This study
	ERK2-F	tgtgttgctccttctctcg	This study
	ERK2-R	tcgcctgtaaaaggacttc	This study
	<b>DNA sequencing primer</b>	$\beta$ -Actin-S	gaacagccttcttagcaccg
CaMKII $\alpha$ -S		agccctagtcccagcctaa	This study
ERK2-S		aggagtgaaggccaagaag	This study

**Table S3. Oligonucleotide Sequences , Related to Figures 1 and 2**